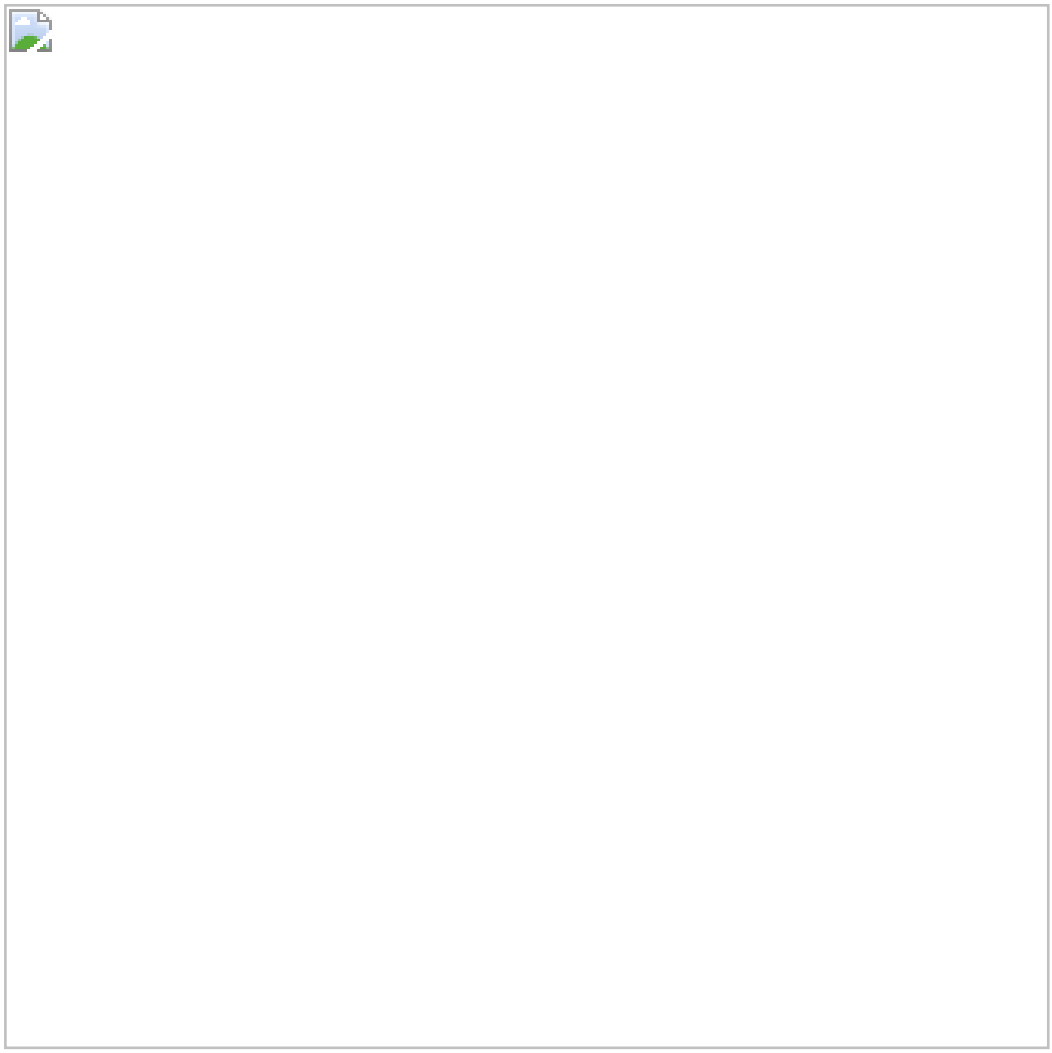

Generation of Reactive Oxygen Species from Silicon Nanowires

Authors: Leonard, Stephen S., Cohen, Guy M., Kenyon, Allison J., Schwegler-Berry, Diane, Fix, Natalie R., et al.

Source: Environmental Health Insights, 8(s1)

Published By: SAGE Publishing

URL: https://doi.org/10.1177/EHI.S15261

Libertas Academica
FREEDOM TO RESEARCH

Open Access: Full open access to this and thousands of other papers at http://www.la-press.com.

Environmental Health Insights

Supplementary Issue: Occupational Health and Industrial Hygiene

Generation of Reactive Oxygen Species from Silicon Nanowires

Stephen S. Leonard[1], Guy M. Cohen[2], Allison J. Kenyon[1], Diane Schwegler-Berry[1], Natalie R. Fix[1], Sarunya Bangsaruntip[2] and Jenny R. Roberts[1]

[1]National Institute for Occupational Safety and Health, Pathology and Physiology Research Branch, Morgantown, WV, USA. [2]IBM T.J. Watson Research Center, Yorktown Heights, NY, USA.

ABSTRACT: Processing and synthesis of purified nanomaterials of diverse composition, size, and properties is an evolving process. Studies have demonstrated that some nanomaterials have potential toxic effects and have led to toxicity research focusing on nanotoxicology. About two million workers will be employed in the field of nanotechnology over the next 10 years. The unknown effects of nanomaterials create a need for research and development of techniques to identify possible toxicity. Through a cooperative effort between National Institute for Occupational Safety and Health and IBM to address possible occupational exposures, silicon-based nanowires (SiNWs) were obtained for our study. These SiNWs are anisotropic filamentary crystals of silicon, synthesized by the vapor–liquid–solid method and used in bio-sensors, gas sensors, and field effect transistors. Reactive oxygen species (ROS) can be generated when organisms are exposed to a material causing cellular responses, such as lipid peroxidation, H_2O_2 production, and DNA damage. SiNWs were assessed using three different *in vitro* environments (H_2O_2, RAW 264.7 cells, and rat alveolar macrophages) for ROS generation and possible toxicity identification. We used electron spin resonance, analysis of lipid peroxidation, measurement of H_2O_2 production, and the comet assay to assess generation of ROS from SiNW and define possible mechanisms. Our results demonstrate that SiNWs do not appear to be significant generators of free radicals.

KEYWORDS: reactive oxygen species, nanomaterials, nanotoxicology, free radicals, silicon

SUPPLEMENT: Occupational Health and Industrial Hygiene

CITATION: Leonard et al. Generation of Reactive Oxygen Species from Silicon Nanowires. *Environmental Health Insights* 2014:8(S1) 21–29 doi: 10.4137/EHI.S15261.

RECEIVED: August 28, 2014. **RESUBMITTED:** September 25, 2014. **ACCEPTED FOR PUBLICATION:** September 26, 2014.

ACADEMIC EDITOR: Timothy Kelley, Editor in Chief

TYPE: Original Research

FUNDING: This study was funded by the NIOSH National Occupation Research Agenda project "Potential effects of silicon-based nanowires on lung toxicity." The findings and conclusions of this paper have not been formally disseminated by NIOSH and should not be construed to represent any agency determination or policy. Mention of any brand name does not constitute product endorsement. The authors confirm that the funder had no influence over the study design, content of the article, or selection of this journal.

COMPETING INTERESTS: Authors disclose no potential conflicts of interest.

CORRESPONDENCE: SEL5@CDC.GOV

Paper subject to independent expert blind peer review by minimum of two reviewers. All editorial decisions made by independent academic editor. Upon submission manuscript was subject to anti-plagiarism scanning. Prior to publication all authors have given signed confirmation of agreement to article publication and compliance with all applicable ethical and legal requirements, including the accuracy of author and contributor information, disclosure of competing interests and funding sources, compliance with ethical requirements relating to human and animal study participants, and compliance with any copyright requirements of third parties. This journal is a member of the Committee on Publication Ethics (COPE).

Introduction

Nanomaterials are being produced in greater quantities every day and the diversity of the materials and finished products incorporating these nanoparticles is expanding.[1–3] Nanoparticles are defined by the National Institute for Occupational Safety and Health (NIOSH) Nanotechnology Research Center as particles that have at least one dimension between 1 and 100 nm. At this size, materials begin to exhibit unique properties that affect physical, chemical, electronic, and biological behavior. Nanomaterials are generally defined as engineered structures, devices, and systems created from nanoparticles. Nanoparticles are being used in medicine to deliver vaccines and to increase bone growth around dental or joint implants.[4,5] Nanoparticles can be dispersed in industrial coatings to protect wood, plastic, and textiles from exposure to UV rays, and in fabric, they are used to kill bacteria, making clothing odor resistant.[6] Environmental applications range from breakdown of oil into biodegradable compounds as a catalyst to breakdown of volatile organic pollutants in air and to clean up carbon tetrachloride pollution in ground water.[7,8] In energy and electronics, they are used in development of low-cost electrodes for fuel cells, and ink-containing nanoparticles are used to form conductive lines in circuit boards.[9] Nanomaterials are no longer a "high tech" innovation but are entering

not only the medical and scientific world but also in every day consumer items. This has led to an impact of up to $1 trillion on the worldwide economy and as many as 2 million people employed in manufacturing.[3] The fast growth of nanotechnology has led to concerns about worker safety and exposure to these new materials both in chemical composition and physical characteristics.[10–13] Toxicology studies already completed have shown a variety of results depending on a material's physicochemical make-up, the route of exposure, and the level of exposure.[10,14–16] Research has also demonstrated that there are differences in the *in vitro* and *in vivo* toxicities of the same particles.[17–19]

The present investigation represents a cooperative research effort between NIOSH and IBM to investigate possible free radical generation from reactions involving silicon nanowires (SiNWs). Single-crystal SiNWs were synthesized by IBM T.J. Watson Research Center using the vapor–liquid–solid method with silane as the silicon precursor and gold as the catalyst. Diameters of SiNWs range from ~20 to 30 nm and length was ~15 μm. Each wire had a uniform diameter, with <1 nm change along the length of a wire. A gold nanoparticle was used to catalyze the growth of the wire in the form of an Au–Si eutectic particle. As detailed in the Method section, each SiNW consists of a silicon core and a thin silicon dioxide shell. In addition, at one end of the wire, there is a gold nanoparticle, which was the catalyst for the nanowire growth.

In this study, we tested SiNWs with a diameter of 20–30 nm and lengths of 100–1000 nm. Since SiNW readily forms a thin, native silicon oxide shell in air or water, and silicon oxide is found abundantly in nature and is relatively nontoxic, SiNWs are expected to be chemically inert. However, their anisotropic morphology could elicit cellular response similar to asbestos. NIOSH considers silicon to be a relatively inert material with a recommended exposure level of 5 mg/m^3 for respirable dust (<10 μm diameter) and 10 mg/mL^3 for total dust.[20] *In vitro* doses ranged from possible workplace exposure levels to the higher unlikely levels in order to develop a dose–response relationship for SiNW-induced free radical responses. Exposure levels of 10–100 μg/mL are frequently used in nanoparticle research, while 250 μg/mL was included as an upper endpoint. Studies on physical characteristics of SiNW are numerous; however, biological studies are few in number and research into basic reactive oxygen species (ROS)/free radical generation is even more limited. Cellular exposures to SiNW have been done in mouse osteoblastic cell lines,[21] osteoblasts,[22] hepatic cell lines,[23] and kidney cells.[24,25] However, these studies have not been performed on wires using the inhalable form, which is more likely to be the type of occupational exposure of concern. One *in vivo* study performed at NIOSH[26] found that SiNW induced an acute toxicity related to increased lung injury and inflammation. Although initial clearance was rapid, the SiNW that remained led to an increase in collagen deposition in the lungs. Another *in vitro* study[27] also demonstrated an inflammatory response; however, it used flat growth surfaces and not free SiNW, which are the likely inhalable fraction. To our knowledge, no studies have been performed to investigate the possible ROS generation from exposure to inhalable SiNW as a potential mechanism for this acute toxicity observed *in vivo*.

The goal of this study was to assess possible free radical and ROS generation from SiNW using several possible initiators. NIOSH considers silicon a relative inert material; therefore, we do not expect to see much chemically derived toxicity from the SiNW. SiNWs were detached from the growth wafer, suspended in dispersion media (DM),[28] and sonicated. Characterization of the resulting particles was also performed. SiNWs were then exposed to H_2O_2 to measure generation of hydroxyl radicals (·OH) by a Fenton-like reaction.[29] RAW 264.7 mouse monocyte macrophages were also exposed to SiNW to measure the ROS generation and effects on a cellular system that has shown radical generation after particle exposure in previous studies.[30,31] Naïve and pre-exposed rat alveolar macrophages (AMs) were also assessed for ROS formation in order to determine immediate and primed responses to SiNW exposure. Possible downstream effects and damage caused by ROS generation were also investigated using measurement of H_2O_2 generation, lipid peroxidation, and DNA damage using exposed RAW 264.7 cells. Generation of ROS and cellular damage due to ROS can initiate respiratory burst in cells and lead to further activation of ROS signaling pathway and cytokine release.[32–34]

Methods

Reagents. Chelex 100 resin was purchased from Bio-Rad Laboratories (Richmond, CA). Phosphate-buffered saline (PBS) [KH_2PO_4 (1.06 mM), Na_2HPO_4 (5.6 mM), NaCl (154 mM), pH 7.4] was purchased from Biowhittaker Inc. (Walkersville, MD). The PBS was treated with Chelex 100 to remove transition metal ion contaminants. Dulbecco's modified eagles medium (DMEM), 5,5-dimethyl-1-pyroline-oxide (DMPO), fetal bovine serum (FBS), $FeSO_4{\cdot}H_2O_2$, and penicillin/streptomycin were purchased from Sigma-Aldrich Chemical Company (St. Louis, MO, USA). The spin trap, DMPO, was purified by charcoal decolorization and vacuum distillation and was free of electron spin resonance (ESR) detectable impurities. Quartz sample tubes were purchased from Wilmad Glass (Buena, NJ). Particles used in comparison studies were Min-U-Sil (U.S. Silica Co., Berkeley Springs, WV), commercially manufactured raw multi- and single-walled carbon nanotubes (MWCNT and SWCNT, respectively), in collaboration with the National Institute of Standards and Technology (Gaithersburg, MD), UICC standard crocidolite asbestos (SPI Supplies, West Chester, PA),

titanium dioxide (TiO_2) nanoparticles (AEROXIDE TiO_2 P25; Degussa AG, Dusseldorf, Germany), and amosite (Transvaal, South Africa).

Growth of SiNWs. SiNWs were grown and synthesized by IBM T.J. Watson Research Center using the vapor–liquid–solid (VLS) method.[35] A thin (2 nm) film of gold was deposited on a clean Si wafer. After annealing the substrate at 450° C in a growth chamber, the gold film agglomerated into individual nanoparticles. Silane (SiH_4) gas was then blown over the substrate to start the SiNW growth. The nanoparticle catalyzed the SiNW formation by decomposing the silane and incorporating Si into the catalyst to form an Au–Si eutectic droplet. When Si became supersaturated, it precipitated out of the droplet into crystalline solid. The diameter of the nanowires was therefore defined by the size of this eutectic droplet. This led to an anisotropic formation of SiNW as the droplet moved up and away from the substrate as the nanowire grew (Fig. 1). The length of the SiNWs was controlled by the growth time. When the growth terminated and the substrate cooled down, the gold catalysts separated back out at the tips. A dense growth of these nanowires is shown in Figure 2A, having an average diameter of approximately 25 nm. Note that native, thin oxide shells automatically form when the SiNWs are exposed to air or an aqueous solution.

Morphology of SiNW particles by transmission electron microscopy. Wafers were cut (etched and broken) along cleavage planes. Chips were then placed in containers with EtOH and sonicated for one minute (6× EtOH removal and replacement). SiNWs were the same material used by Roberts et al.[26] After evaporation of the EtOH, wires were resuspended in a known volume of sterile PBS and an aliquot was removed for weight measurement and imaging by field emission scanning electron microscopy (FESEM). Images were collected on a Hitachi (Tokyo, Japan) S-4800 FESEM (Fig. 2B). Aggregation of the wires was found; therefore, wires were further sonicated in DM 28 consisting of 0.6 mg/mL rat serum albumin, 0.01 mg/mL dipalmitoylphosphatidylcholine, and sonicated for 5 min at 10 watts power, which dispersed the wire aggregations, providing wires that were 70% <5 µm and 30% >5 µm to be used in experiments. Elemental analysis for Au was performed by North Carolina State University Nuclear Reactor Program, Department of Nuclear Engineering (Raleigh, NC) using neutron activation. SiNW samples and standards were irradiated in a PULSTAR reactor

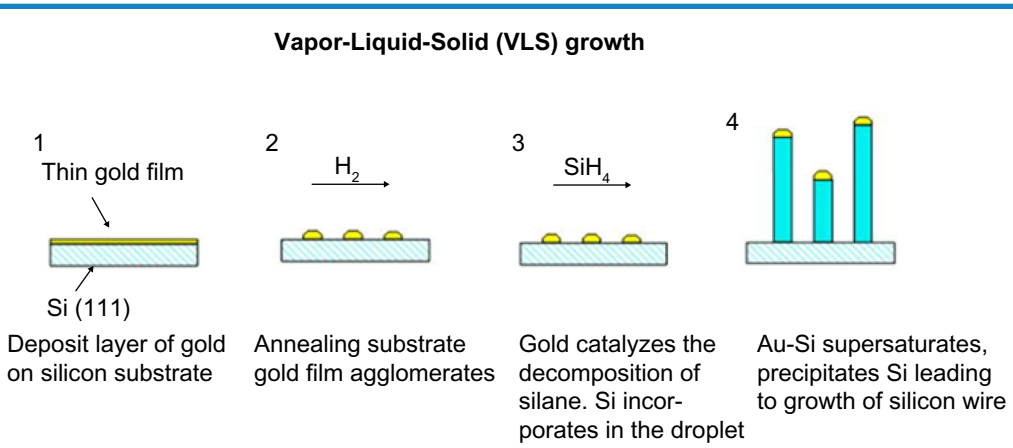

Figure 1. SiNW growth via the vapor–liquid–solid method with gold nanoparticles. (**1**) A thin layer of gold is deposited on silicon substrate. (**2**) The substrate is annealed to form individual gold nanoparticles. (**3**) Gold nanoparticles catalyzes the decomposition of silane gas and incorporate Si into Au–Si eutectic droplets. (**4**) Supersaturated Si participated out of the droplets, forming anisotropic nanowires, having the same diameters as the gold nanoparticles.

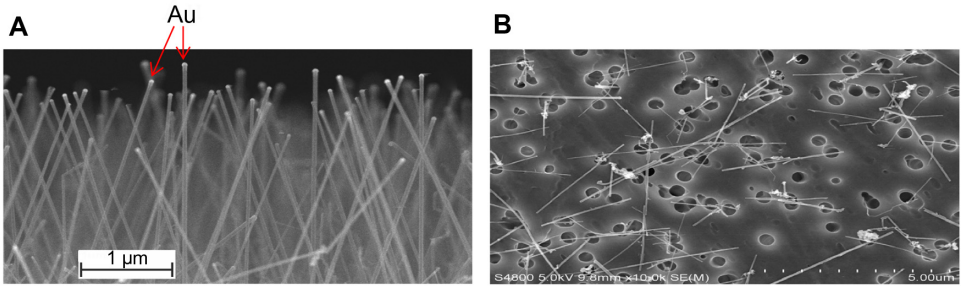

Figure 2. Scanning electron images of SiNW. (**A**) Image of SiNWs still attached to the growth wafer. Gold nanoparticles that catalyzed the anisotropic growth can be seen at the tips of each SiNW. (**B**) Image of harvested SiNWs re-deposited on a substrate for viewing (SiNWs were removed from the growth wafer, filtered, and re-suspended in dispersion media to prevent aggregation). Note that the circular holes are features of the substrate itself.

rotating exposure port for 12 minutes. After one week, these were counted for one hour each on a gamma spectroscopy system and analyzed for Au.[36,37] Length distribution of SiNW was determined using 20 micrographs of SiNW suspended and sonicated in DM and imaged using FESEM at 5–20 kV. A total of 730 nanowires were counted, after which the length of each was measured using Gundersen's unbiased counting rules[38] to determine length frequency and distribution. In addition, micrographs of SiNW before and after sonication in DM were compared to assess potential wire breakage resulting from preparation of the NW suspension.

Cell culture. RAW 264.7 mouse peritoneal monocytes were purchased from American Type Culture Collection (Rockville, MD). RAW 264.7 cells are commonly used and have been found to respond to particle exposure in a manner similar to primary AM.[31,39,40] RAW 264.7 cells were cultured in DMEM with 10% FBS, 2 mM L-glutamine, and 50 mg/mL penicillin/streptomycin at 37 °C in a 5% CO_2 in air incubator. Cells were split after confluence approximately for every three days. Trypan blue assay was used to determine cell viability.

Free radical measurements. ESR and spin trapping were used to detect short-lived free radical intermediates. Hydroxyl radicals were measured using the addition-type reaction of a short-lived radical with a compound (spin trap) to form a relatively long-lived paramagnetic free radical product (spin adduct), which can then be studied using conventional ESR. Concentrations given in the figure legends are final concentrations. The intensity of the signal is used to measure the relative amount of short-lived radicals trapped, and the hyperfine couplings of the spin adduct are characteristic of the original trapped radicals. Spin trapping is the method of choice for detection and identification of free radical generation because of its specificity and sensitivity. All ESR measurements were conducted using a Bruker EMX spectrometer (Bruker Instruments Inc., Billerica, MA) and a flat cell assembly. Hyperfine couplings were measured (to 0.1 G) directly from magnetic field separation using potassium tetraperoxochromate (K_3CrO_8) and 1,1-diphenyl-2-picrylhydrazyl as reference standards.[41,42] The relative radical concentration was estimated by multiplying half of the peak height by $(\Delta H_{pp})^2$, where ΔH_{pp} represents peak-to-peak width. The Acquisit program was used for data acquisitions and analyses (Bruker Instruments Inc.). Preliminary investigations demonstrated that the presence of Au (10% by weight) on the nanowires did not significantly affect the production of ROS (data not shown).

Hydroxyl radical production from H_2O_2. SiNW in concentrations shown in figure legends and the spin trap DMPO (100 mM) were mixed in test tubes at a final volume of PBS in the presence of 1 mM H_2O_2. The reaction mixture was then transferred to a quartz flat cell for ESR measurement three minutes after nanowires exposure. Experiments were performed at room temperature and in ambient air.[29]

Hydroxyl radical production from exposed RAW Cells. RAW 264.7 cells (10^6), DMPO (200 mM), and SiNWs (final concentrations are listed in the figure legends) were mixed in test tubes containing PBS to a final volume of 1 mL. The reaction mixture was allowed to incubate at 37 °C for 10 min and then transferred to a flat cell for ESR measurement. Experiments were performed at room temperature and in ambient air.[29,43]

Rat AM recovery. Naïve Male Sprague-Dawley [Hla: (SD) CVF] rats from Hilltop Lab Animals, Inc. (Scottdale, PA), weighing 250–300 g and free of viral pathogens, parasites, mycoplasmas, Helicobacter, and CAR bacillus, were used for macrophage harvests. The rats were acclimated for at least 6 days after arrival and were housed in ventilated polycarbonate cages on Alpha-Dri cellulose chips and hardwood Beta-chips as bedding and provided HEPA-filtered air, irradiated Teklad 2918 diet, and tap water ad libitum when not being exposed. The animal facilities are specific pathogen-free, environmentally controlled, and accredited by the Association for Assessment and Accreditation of Laboratory Animal Care International.

Rat intratracheal instillation (IT) was performed on day 0 after light anesthetization following intraperitoneal injection of a 1% sodium methohexital solution (Brevital; Eli Lilly, Indianapolis, IN). Rats were instilled intratracheally with 10, 50, and 250 μg of SiNW in DM. Control rats received the same volume (300 mL) of sterile DM. Rats were then deeply anesthetized at 1, 3, and 7 days postadministering an intraperitoneal injection of sodium pentobarbital (N100 mg/kg body weight; Butler Co., Columbus, OH) and then exsanguinated by severing the abdominal aorta. Macrophages were harvested via lavage with 6 mL aliquots of PBS until 30 mL were collected. These samples also were centrifuged for 10 min at 500 × g and the cell-free BALF was discarded. The cell pellets from all washes for each rat were combined, washed, and resuspended in 1 mL of PBS and recovered macrophages were then exposed to SiNWs, served as control cells, or used directly for ESR measurement of ROS, pre-exposed cells.[26]

H_2O_2 production. H_2O_2 production was monitored using a Bioxytech quantitative hydrogen peroxide assay kit (H_2O_2-560; Oxis International Inc., Portland, OR). Measurements were made on a system containing 5×10^6 RAW 264.7 mouse peritoneal monocytes/milliliter in pH 7.4 PBS and exposing them to nanowires. RAW 264.7 cells were exposed to the various concentrations of nanowires for 30 minutes in a 37 °C incubator. Absorbance was monitored at a wavelength of 560 nm using a Spectra Max 250 multi-well plate reader (Molecular Devices, Sunnyvale, CA).[30,43]

Lipid peroxidation. Lipid peroxidation of RAW 264.7 mouse peritoneal monocytes was measured using a colormetric assay for malondialdehyde (LPO-586; Oxis International Inc., Portland, OR). A reaction mixture contained nanowires and 10^7 cells in a total volume of 1 mL PBS (pH 7.4). A Fenton reaction, $FeSO_4$ (1 mM), H_2O_2 (1 mM), and 10^7 cells, was also carried out as a positive control (data not shown). RAW 264.7 mouse cells were exposed to the various

concentrations of nanowires for 1 hour in a shaking water bath at 37 °C. The measurement of lipid peroxidation is based on the reaction of a chromogenic reagent with malonaldehyde at 45 °C. The absorbance of the supernate was measured at 586 nm.[44,45]

DNA damage: comet assay. The comet assay was performed using methods described in the assay kit (CometAssay®; Trevigen, Gaithersburg, MD). A typical reaction mixture contained nanowires and 10^7 RAW 264.7 mouse peritoneal monocytes cells brought to a total volume of 1 mL in PBS (pH 7.4). Briefly (all steps performed in the dark or low light conditions), RAW 264.7 mouse cells were exposed to various concentrations of nanowires and incubated in media at 37 °C for 1 hour. The cells were washed (2 ×) with PBS, combined with LMAgarose, and then pipetted onto a comet slide. The slides were refrigerated for 30 minutes, immersed in lysis solution, chilled for 60 minutes, and then immersed in alkaline solution for 55 minutes. These were then placed in a horizontal electrophoresis chamber for 40 minutes at 300 mA. The slides were washed and SYBR green stain was then added. The slides were visualized using fluorescence microscopy, with an image capturing system (Olympus AX70 and sample PCI; Compix Inc, Cranberry Township, PA). A minimum of 50 cells were scored for each sample at 400 × magnification. The distance between the edge of the head and the end of the tail was measured using an automated image analysis system (Optimas 6.51; Media Cybernetics Inc, Silver Spring, MD).[46,47]

Statistics. Data were expressed as mean ± standard error of the mean (SEM), $n = 4$ for each group. One-way ANOVA test was performed to determine significant difference among treatment groups using SigmaStat statistical software (Jandel Scientific, San Rafael, CA) to compare the responses between treatments. For toxicity studies, significant differences among groups were assessed by the Student–Newman–Keuls method. Statistical significance was set at $P < 0.05$.

Results

Radical production from exposure to H_2O_2. Figure 3 shows the results of measurement of ·OH generation after reaction of SiNW (25 and 50 µg/mL) with H_2O_2 (10 mM) in the presence of the free radical spin trap DMPO (100 mM) for three minutes. ESR settings are given in figure legends. No significant differences in generation of ·OH radical were observed for either concentration. SiNWs were generated under strictly controlled conditions and with minimum contaminants, such as transition metals, which could react with H_2O_2 and cause the generation of radicals.

Radical production after exposure to RAW 264.7 cells. Figure 4 shows the results of measurement of free radical generation after reaction of SiNW (25 and 50 µg/mL) with RAW 264.7 mouse monocyte macrophages (10^6/mL) in the presence of the free radical spin trap DMPO (200 mM) after incubation for five minutes at 37 °C. ESR settings are given in figure legends. A significant difference was observed

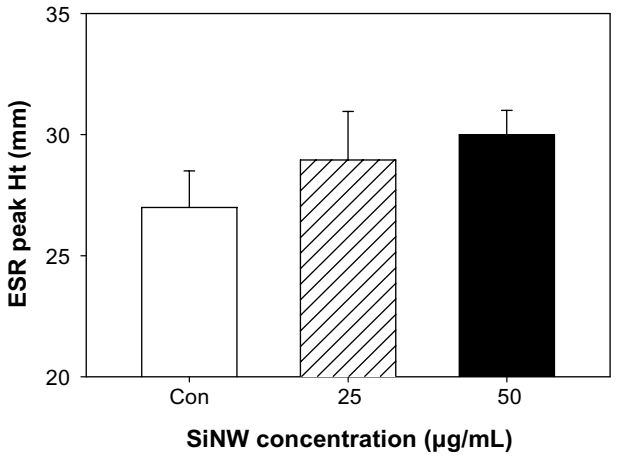

Figure 3. Acellular reactivity of SiNW. ESR spectra recorded three minutes after reaction initiation, from a pH 7.4 phosphate buffered solution of 100 mM DMPO and the following reactants: SiNW, H_2O_2 (10 mM). The ESR spectrometer settings were: receiver gain, 2.5×10^5; time constant, 0.25 seconds; modulation amplitude, 0.5 G; scan time, 8 minutes; magnetic field, 3375 ± 100 G. The data represent mean ± SEM values of four independent experiments.

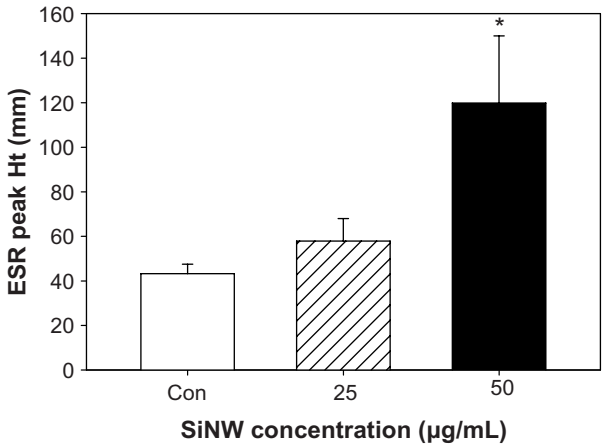

Figure 4. Monocyte reactivity. ESR peak heights recorded after five minutes incubation at 37 °C, from a pH 7.4 phosphate buffered solution of 200 mM DMPO and the following reactants: SiNW, RAW 264.7 cells (10^6/mL). The ESR spectrometer settings were: receiver gain, 2.5×10^5; time constant, 0.25 seconds; modulation amplitude, 0.5 G; scan time, 8 minutes; magnetic field, 3375 ± 100 G. The data represent mean ± SEM values of four independent experiments. *Different from the control ($P < 0.05$).

in the 50 µg/mL exposure group, demonstrating a possible reaction from cells and a respiratory burst response. As noted above, SiNWs were generated under strictly controlled conditions and with minimum contaminants, such as metals, which indicates that the nanowires caused reaction was due to their physical characteristics, such as increased surface area, rather than their chemistry. No significant difference was observed in cell viability at the doses used (data not shown).

Radical production after exposure to naïve rat AMs. Figure 5 shows the results of measurement of free radical

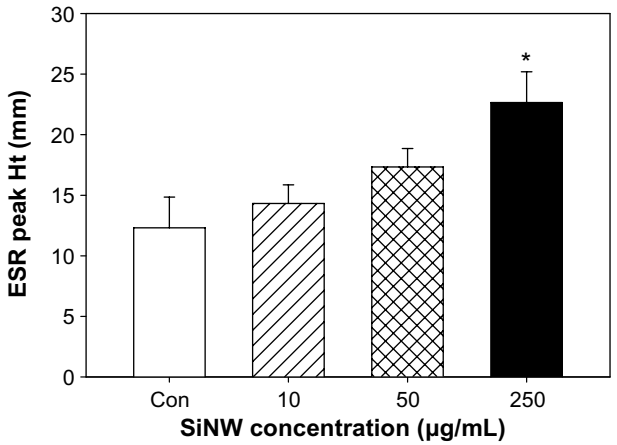

Figure 5. Primary macropage reactivity. ESR peak heights recorded after five minutes incubation at 37 °C, from a pH 7.4 phosphate buffered solution of 200 mM DMPO and the following reactants: SiNW, naïve rat AMs (10^6/mL). The ESR spectrometer settings were: receiver gain, 2.5×10^5; time constant, 0.25 seconds; modulation amplitude, 0.5 G; scan time, 8 minutes; magnetic field, 3375 ± 100 G. The data represent mean ± SEM values of four independent experiments. *Different from the control ($P < 0.05$).

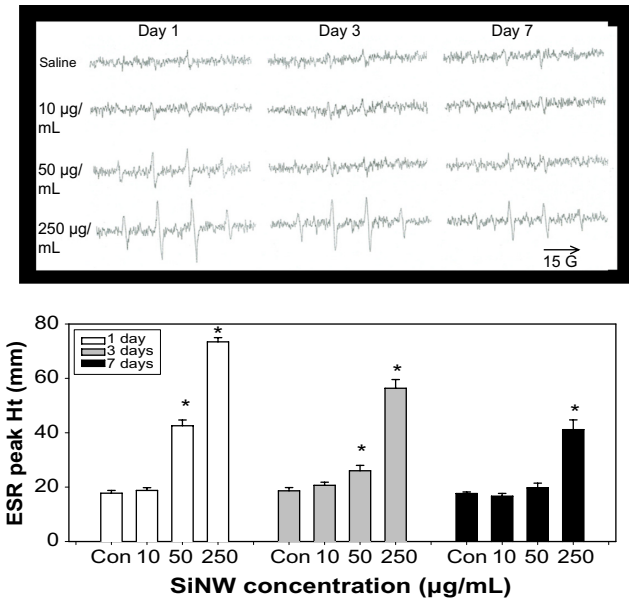

Figure 6. Reactivity *ex vivo*. ESR peak heights recorded after five minutes incubation at 37 °C, from a pH 7.4 phosphate buffered solution of 200 mM DMPO and the following reactants: pre-exposed rat AMs (10^6/mL). The ESR spectrometer settings were: receiver gain, 2.5×10^5; time constant, 0.25 seconds; modulation amplitude, 0.5 G; scan time, 8 minutes; magnetic field, 3375 ± 100 G. The data represent mean ± SEM values of four independent experiments. *Different from the control ($P < 0.05$).

generation after reaction of SiNW (25, 50, and 250 µg/mL) with rat AMs from naïve rats. The macrophages (10^6/mL) were exposed to the nanowires after incubation for five minutes at 37 °C in the presence of the free radical spin trap DMPO (200 mM). ESR settings are given in figure legends. A significant difference was observed at the 250 µg/mL exposure group and with minimum contaminants, such as metals. This indicates that the nanowires caused reaction was due to their physical characteristics rather than their chemistry.

Radical production of rat AMs after IT exposure to nanowires. Rats that were pre-exposed to SiNWs were then lavaged, and the harvested rat AMs were analyzed for radical production using ESR measurement. Rats were then exposed to 10, 50, and 250 µg of SiNW in DM. Macrophages were harvested at 1, 3, and 7 days post-exposure time points. Figure 6 shows that macrophages produced more radicals at the earlier time points, 1 and 3 days, than at 7 days. Significant increases were seen in both the 50 and 250 µg exposures in the 1 and 3 day post-exposure cells, while the 10 µg dose did not result in significant radical formation at any time point.

H_2O_2 production in exposed RAW 264.7 cells. Figure 7 shows the generation of H_2O_2 from RAW 264.7 mouse monocyte macrophages (5×10^6/mL) after exposure to SiNWs and incubated for 30 minutes at 37 °C. A significant increase in H_2O_2 was observed at the 500 µg/mL exposure. These results demonstrate the activation of a cellular respiratory burst, via the increased production of H_2O_2 at the highest concentration of SiNWs.

Lipid peroxidation in exposed RAW 264.7 cells. Lipid peroxidation results shown in Figure 8 revealed a significant increase in malondialdehyde at the 500 µg/mL concentration after incubating RAW 264.7 cells with SiNWs for one hour. Malondialdehyde forms as a result of ROS degrading polyunsaturated lipids in the cellular lipid bilayer. These results also demonstrate generation of and damage created by ROS from exposed cells; however, these results were only observed in the highest concentration of SiNW.

DNA damage in exposed RAW 264.7 cells. As shown in Figure 9, a significant increase in tail length (DNA damage) at the 500 µg/mL concentration occurred after incubating

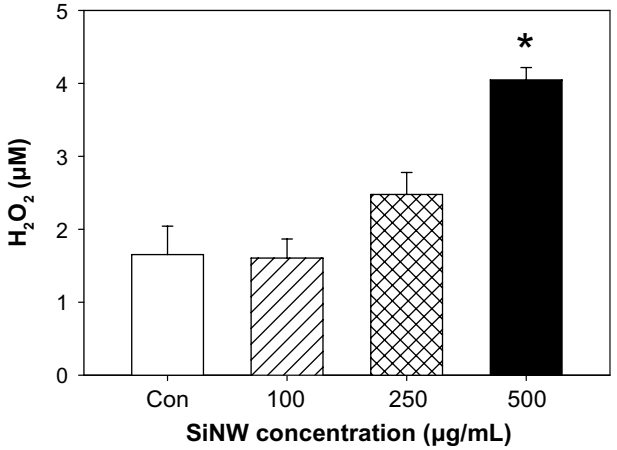

Figure 7. H_2O_2 production in incubation mixtures containing 5×10^6 RAW 264.7 cells alone, and after exposure to 100, 250, and 500 µg/mL SiNW. The data represent mean ± SEM values of five independent experiments. *Different from the control ($P < 0.05$).

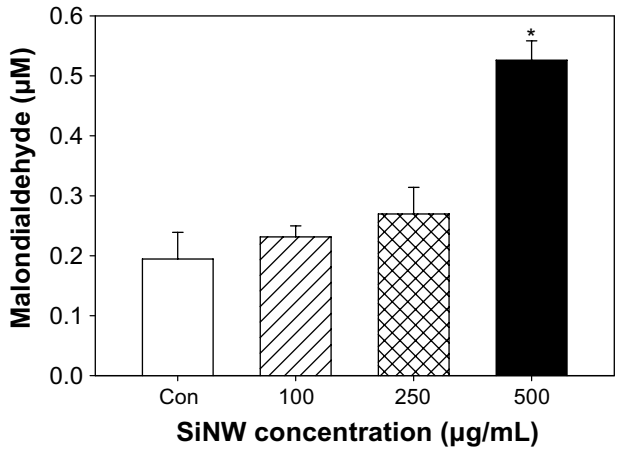

Figure 8. SiNW-induced lipid peroxidation. Exposure mixtures contained 5×10^7 RAW 264.7 cells and 0, 100, 250, or 500 µg/mL SiNW. The data represent mean ± SEM values of five independent experiments. *Different from the control ($P < 0.05$).

RAW 264.7 cells with SiNWs for one hour. Increase in tail length is due to DNA being fragmented as a result of ROS production. These results also demonstrated generation of and damage created by ROS from exposed cells and nuclear material; however, these results were only observed using the highest concentration of SiNW.

Comparison of SiNW with other materials. Figure 10 illustrates a general comparison of results obtained using other previously tested materials following measurement of ·OH generation after reaction of the particle with H_2O_2 (10 mM) in the presence of the free radical spin trap DMPO (100 mM) for three minutes. SiNWs were compared with TiO_2, amosite, SWCNT both purified (P) and unpurified (UP), and Min-U-Sil. Although not all materials are nanomaterials, a general comparison of reactivity shows that SiNW did not cause significant generation of ·OH on reaction with H_2O_2 while unpurified SWCNT and Min-U-Sil did generate a significant amount.

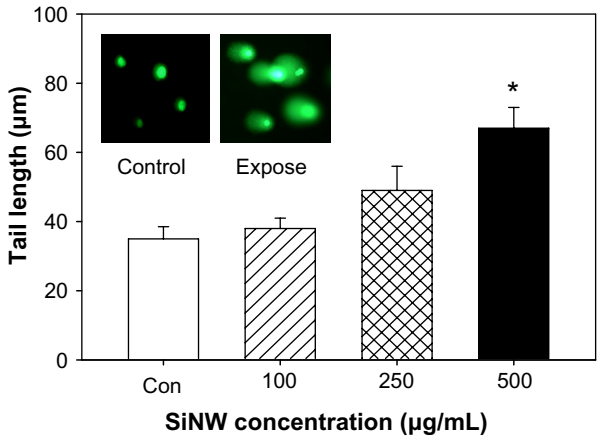

Figure 9. DNA damage in RAW 264.7 cells induced by SiNW as measured by the CometAssay. An increase in tail length represents increased DNA damage. Inset A shows control cells, inset B shows 500 µg/mL exposed cells. Data presented are means of ±SEM for five sets of experiments at least 50 tail counts per experiment. *Significant increase in DNA damage compared to control cells ($P < 0.05$).

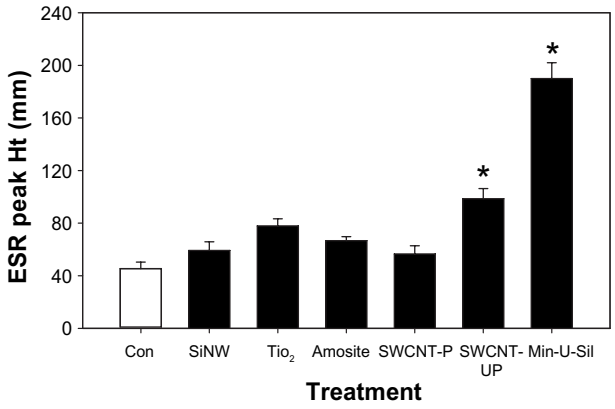

Figure 10. A comparison of ability of SiNWs to induce ROS. ESR spectra recorded three minutes after reaction initiation, from a pH 7.4 phosphate buffered solution of 100 mM DMPO and the following reactants: H_2O_2 (10 mM) and 50 µg/mL of SiNW, TiO_2, amosite, SWCNT-P (purified), SWCNT-UP (unpurified), or Min-U-Sil. The ESR spectrometer settings were: receiver gain, 2.5×10^5; time constant, 0.25 seconds; modulation amplitude, 0.5 G; scan time, 8 minutes; magnetic field, 3375 ± 100 G. The data represent mean ± SEM values of four independent experiments. *Different from the control ($P < 0.05$). Note that peak height of SiNW is different from Figure 3A because of changed scale in order to compare with other samples.

Discussion

Toxicity of nanomaterials is becoming a concern due to the rapid introduction of new materials used and characteristics related to their manufacture. A number of different factors can play a role in nanomaterial toxicity; our investigation examined the possible role of free radical generation in SiNW toxicity. Studies of other high aspect ratio materials, such as asbestos,[48–50] SWCNT,[51,52] and MWCNT,[50] have demonstrated a wide variety of results. These results depended on the cell type used, purity of the material, surface chemistry, accessibility of particle surface, and particle dimensions. Most of the toxicity measured in the high aspect ratio nanomaterials *in vitro* has been related to impurities found on the materials. SWCNT and MWCNT were both found to generate ·OH, but when the particles were purified, the production of these radicals were not significant.[53] The SiNW used in our study had a high aspect ratio with a diameter of 25 nm with 70% of them being <5 µm long and the other 30% were >5 µm long. This anisotropic characteristic creates a large surface area for possible free radical generation upon reaction with initiators. Material >15 µm in length can also cause frustrated phagocytosis in macrophages,[54] which can lead to respiratory burst and generation of a variety of free radicals and ROS.[31,33]

In vitro doses ranged from possible workplace exposure levels to the higher unlikely levels in order to develop a

dose–responsive relationship for SiNW-induced free radical responses. Exposure levels of 10–100 μg/mL are frequently used in nanoparticle research, while 250 μg/mL is the upper end of most exposure studies.[26,55,56] The goal of our study was to establish the dose at which SiNW elicited a response. Intratracheal dosages used in our study were actually relatively low when compared to carbon nanotube (CNT) exposures in rats in published reports. Our highest dosage of 250 μg equates to 1 mg/kg of body weight. In comparison to studies done with CNT by Warheit et al.[55] (using up to 5 mg/kg body weight) and Aiso et al.[56] (ranging from 40 to 160 μg per rat), the doses used here were substantially lower.

Our investigation examined the ability of SiNW to generate radicals from a "Fenton-like" reaction with H_2O_2, cultured RAW 264.7 cells that have been used in other studies, and rat AMs, both naïve and exposed. SiNW did not significantly increase ·OH radicals produced upon reaction with H_2O_2 at any concentration, indicating that the SiNWs are free from reactive impurities such as contaminating transition metals, such as Fe, which could initiate generation of ·OH and reactive zones such as fracture planes found in freshly ground silica.[30] A significant increase in radical production was observed at the 50 μg/mL concentration in RAW 264.7 cells exposed to SiNWs, which may indicate a respiratory burst upon the cells interacting with SiNW, leading to activation of phagocytosis. Free radical production also occurred after naïve lavaged rat AMs were exposed to SiNWs, as significant radical production measurement at the 250 mg/mL exposure level in the pre-exposed rat AM resulted in a different response. After rats were exposed intratracheally to SiNWs and macrophages were harvested at 1, 3, and 7 days post-exposure, ·OH production was increased after administering 50 and 250 μg/mL exposure levels after 1 and 3 days. However, at 7-day time point, only the 250 μg/mL exposure level elicited a response, indicating that these cells were primed for a response and a persistent production of radicals lasted up to 7 days. The decrease in radical production over time shows that the rat AMs are became less responsive, perhaps due to the wires being cleared from the alveolar space or being completely phagocytized.

Downstream ROS initiated damage was assessed by measuring H_2O_2 generation, lipid peroxidation, and DNA damage. H_2O_2 generation in exposed RAW 264.7 cells increased only at the 500 μg/mL exposure level. Lipid peroxidation and DNA damage also increased only at the 500 μg/mL exposure level. ROS damage occurred only after the 500 μg/mL exposure level was administered, which is higher than most experimental exposure levels for nanoparticles. This high exposure level was included to determine whether damage could occur under overload lung conditions. However, at more work place-related levels of 100 μg/mL and 250 μg/mL, no significant increase in ROS-initiated damage resulted. Although cells seem to respond with an initial ROS release upon encountering SiNW, over time, ROS production decreases. SiNWs do not appear to stimulate free radical generation *in vitro* to a significant degree and cause an oxidative burst only transiently *in vivo*. Further investigations and comparisons of SiNWs with other materials at the same concentrations are presently underway.

While ROS-related toxicity was not seen at the lower occupational levels of exposures and NIOSH does not consider silicon of special concern, the results from the study by Roberts et al.[26] suggest that workers should take precautions while working with this material and limit their exposure level. ROS and ROS-related damage do not appear to be the method of SiNW toxicity.

Author Contributions

Conceived and designed the experiments, wrote the manuscript, performance of ESR and analysis of all data: SSL. Generation of SiNW, analysis of characteristics, methods: GC, SB. *In vitro* cell culture, generation of ESR, H_2O_2, lipid peroxidation and DNA damage data: AJK, NRF. Electron microscopy: DSB. *In vivo* rat instillation and harvesting of cells, co-investigator on project: JRR. All authors reviewed and approved final manuscript.

REFERENCES

1. Maynard AD. Nanotechnology: the next big thing, or much ado about nothing? *Ann Occup Hyg*. 2007;51:1–12.
2. Oberdorster G, Oberdorster E, Oberdorster J. Nanotoxicology: an emerging discipline evolving from studies of ultrafine particles. *Environ Health Perspect*. 2005;113:823–39.
3. NIOSH. Approaches to Safe Nanotechnology: Managing the Health and Safety Concerns Associated with Engineered Nanomaterials (Pub. No. 2009–125). Atlanta: Department of Health and Human Services, Centers for Disease Control and Prevention, National Institute for Occupational Safety and Health; March 2009.
4. Shvedova AA, Kisin ER, Porter D, et al. Mechanisms of pulmonary toxicity and medical applications of carbon nanotubes: two faces of Janus? *Pharmacol Ther*. 2009;121(2):192–204.
5. Zhao J, Castranova V. Toxicology of nanomaterials used in nanomedicine. *J Toxicol Environ Health B*. 2011;14:593–632.
6. Abramova OV, Gedankenb A, Koltypinb Y, et al. Pilot scale sonochemical coating of nanoparticles onto textiles to produce biocidal fabrics. *Surf Coat Technol*. 2009;204(5):718–22.
7. Chalew TEA, Ajmani GS, Huang H, Schwab KJ. Evaluating nanoparticle breakthrough during drinking water treatment. *Environ Health Perspect*. 2013; 121(10):1161–6.
8. Dhermendra K, Tiwari J. Application of nanoparticles in waste water treatment. *World Appl Sci J*. 2008;3(3):417–33.
9. Raimondi F, Günther G, Scherer G, Kötz R, Wokaun A. Nanoparticles in energy technology: examples from electrochemistry and catalysis. *Angew Chem Int Ed Engl*. 2005;44(15):2190–209.
10. Rushton EK, Jiang J, Leonard SS, et al. Concept of assessing nanoparticle hazards considering nanoparticle dosemetric and chemical/biological response metrics. *J Toxicol Environ Health A*. 2010;73:445–61.
11. Simon-Deckers A, Loo S, Mayne-L'hermite M, et al. Size-composition and shape-dependent toxicological impact of metal oxide nanoparticles and carbon nanotubes toward bacteria. *Environ Sci Technol*. 2009;43:8423–9.
12. Yang H, Liu C, Yang D, Zhang H, Xi Z. Comparative study of cytotoxicity, oxidative stress and genotoxicity induced by four typical nanomaterials: the role of particle size, shape and composition. *J Appl Toxicol*. 2009;29:69–78.
13. Zhao X, Heng BC, Xiong S, et al. In vitro assessment of cellular responses to rod-shaped hydroxyapatite nanoparticles of varying lengths and surface areas. *Nanotoxicology*. 2011;5:182–94.
14. Karlsson HL, Gustafsson J, Cronholm P, Möller L. Size-dependent toxicity of metal oxide particles: a comparison between nano- and micrometer size. *Toxicol Lett*. 2009;188:112–8.
15. Love SA, Maurer-Jones MA, Thompson JW, Lin YS, Haynes CL. Assessing nanoparticle toxicity. In: Cooks RG, Yeung ES, eds. *Annual Review of Analytical Chemistry*. Palo Alto, CA: Annual Reviews; 2012. pp 78.

16. Wu N, Wang J, Tafen de N, et al. Shape-enhanced photocatalytic activity of single-crystalline anatase TiO(2) (101) nanobelts. *J Am Chem Soc*. 2010; 132(19):6679–85.
17. Lu S, Duffin R, Poland C, et al. Efficacy of simple short-term in vitro assays for predicting the potential of metal oxide nanoparticles to cause pulmonary inflammation. *Environ Health Perspect*. 2009;117:241–7.
18. Borm PJ, Robbins D, Haubold S, et al. The potential risks of nanomaterials: a review carried out for ECETOC. *Part Fibre Toxicol*. 2006;14:3–11.
19. Han X, Finkelstein JN, Elder A, Biswas P, Jiang J, Oberdorster G. Dose and response metrics in assessing in vitro and in vivo nanoparticle toxicity. *Toxicologist*. 2009;108(1):410, Abstract No. 174.
20. NIOSH. NIOSH Pocket Guide to Chemical Hazards (Pub. No. 2005–149). Atlanta: Department of Health and Human Services, Centers for Disease Control and Prevention, National Institute for Occupational Safety and Health; September 2005.
21. Xie W, Xie Q, Jin M, et al. The β-SiC nanowires (~100 nm) induce apoptosis via oxidative stress in mouse osteoblastic cell line MC3T3-E1. *Biomed Res Int*. 2014;2014:312901.
22. Brammer KS, Choi C, Oh S. Antibiofouling, sustained antibiotic release by Si nanowire templates. *Nano Lett*. 2009;9(10):3570–4.
23. Qi SJ, Yi CQ, Ji SL, Fong CC, Yang MS. Cell adhesion and spreading behavior on vertically aligned silicon nanowire arrays. *ACS Appl Mater Interfaces*. 2009;1:30–4.
24. Kim W, Ng JK, Kunitake ME, Conklin BR, Yang P. Interfacing silicon nanowires with mammalian cells. *J Am Chem Soc*. 2007;129(23):7228–9.
25. Nagesha DK, Whitehead MA, Coffer JL. Biorelevant calcification and noncytotoxic behavior in silicon nanowires. *Adv Mater*. 2005;17(7):921–4.
26. Roberts JR, Mercer RR, Chapman RS, et al. Pulmonary toxicity, distribution, and clearance of intratracheally instilled silicon nanowires in rats. *J Nanomater*. 2012;2012:398302.
27. Ainslie KM, Tao SL, Popat KC, et al. In vitro inflammatory response of nanostructured titania, silicon oxide, and polycaprolactone. *J Biomed Mater Res A*. 2009;91(3):647–55.
28. Porter D, Sriram K, Wolfarth M, et al. A biocompatible medium for nanoparticle dispersion. *Nanotoxicology*. 2008;2(3):144–54.
29. Leonard SS, Chen BT, Stone SG, et al. Comparison of stainless and mild steel welding fumes in generation of reactive oxygen species. *Part Fibre Toxicol*. 2010;7:32.
30. Vallyathan V, Castranova V, Pack D, et al. Freshly fractured quartz inhalation leads to enhanced lung injury and inflammation: potential role of free radicals. *Am J Respir Crit Care Med*. 1995;152:1003–9.
31. Zhang Y, Fong CC, Wong MS, et al. Molecular mechanisms of survival and apoptosis in RAW 264.7 macrophages under oxidative stress. *Apoptosis*. 2005;10(3):545–56.
32. Kang JL, Moon C, Lee HS, et al. Comparison of the biological activity between ultrafine and fine titanium dioxide particles in RAW 264.7 cells associated with oxidative stress. *J Toxicol Environ Health A*. 2008;71:478–85.
33. O'Neill LA. Immunology: how frustration leads to inflammation. *Sci Signaling*. 2008;320:619.
34. Park E-J, Park K. Oxidative stress and pro-inflammatory responses induced by silica nanoparticles in vivo and in vitro. *Toxicol Lett*. 2009;184:18–25.
35. Meng G, Yanagida T, Nagashima K, et al. Preferential interface nucleation: an expansion of the VLS growth mechanism for nanowires. *Adv Mater Deerfield*. 2009;21(2):153–65.
36. Givargizov EI. *Highly Anisotropic Crystals*. Norwell, MA, USA: Kluwer Academic Publishers; 1986.
37. Patolsky F, Zheng G, Lieber CM. Fabrication of silicon nanowire devices for ultrasensitive, label-free, real-time detection of biological and chemical species. *Nat Protoc*. 2006;1(4):1711–24.
38. Gundersen HJG. Notes on the estimation of the numerical density of arbitrary profiles: the edge effect. *J Microsc*. 1977;111:219–23.
39. Jalava PI, Salonen RO, Hälinen AI, et al. In vitro inflammatory and cytotoxic effects of size-segregated particulate samples collected during long-range transport of wildfire smoke to Helsinki. *Toxicol Appl Pharmacol*. 2006;215(3): 341–53.
40. Leonard SS, Roberts JR, Antonini JM, Castranova V, Shi X. $PbCrO_4$ mediates cellular responses via reactive oxygen species. *Mol Cell Biochem*. 2004; 255(1&2):171–9.
41. Janzen EG, Blackburn BJ. Detection and identification of short-lived free radicals by an electron spin resonance trapping technique. *J Am Chem Soc*. 1968;90:5909–10.
42. Buettner GR. Spin trapping: ESR parameters of spin adducts. *Free Radic Biol Med*. 1987;3:259–303.
43. Leonard SS, Castranova V, Chen BT, et al. Particle size dependent radical generation from Wildland fire smoke. *Toxicology*. 2007;236:103–13.
44. Vaca CE, Wilhelm J, Harms-Ringdahl M. Interaction of lipid peroxidation products with DNA. A review. *Mutat Res*. 1988;195:137–49.
45. Comporti M. Lipid peroxidation and cellular damage in toxic liver injury. *Lab Invest*. 1985;53(6):599–623.
46. Collins AR. The comet assay for DNA damage and repair: principles, applications, and limitations. *Mol Biotechnol*. 2004;26(3):249–61.
47. Botta C, Iarmarcovai G, Chaspoul F, et al. Assessment of occupational exposure to welding fumes by inductively coupled plasma-mass spectroscopy and by the alkaline Comet assay. *Environ Mol Mutagen*. 2006;47(4):284–95.
48. Ji Z, Wang X, Zhang H, et al. Designed synthesis of CeO_2nanorods and nanowires for studying toxicological effects of high aspect ratio nanomaterials. *ACS Nano*. 2012;6:5366–80.
49. Roberts JR, Chapman RS, Tirumala VR, et al. Toxicological evaluation of lung responses after intratracheal exposure to non-dispersed titanium dioxide nanorods. *J Toxicol Environ Health A*. 2011;74:790–810.
50. Pacurari M, Castranova V, Vallyathan V. Single- and multi-wall carbon nanotubes versus asbestos: are the carbon nanotubes a new health risk to humans? *J Toxicol Environ Health A*. 2010;73(5):378–95.
51. Shvedova AA, Kisin ER, Mercer R, et al. Unusual inflammatory and fibrogenic pulmonary responses to single-walled carbon nanotubes in mice. *Am J Physiol Lung Cell Mol Physiol*. 2005;289(5):L698–708.
52. Wang L, Castranova V, Mishra A, et al. Dispersion of single-walled carbon nanotubes by a natural lung surfactant for pulmonary in vitro and in vivo toxicity studies. *Part Fibre Toxicol*. 2010;19(7):31.
53. Kagan VE, Tyurina YY, Tyurin VA, et al. Direct and indirect effects of single walled carbon nanotubes on RAW 264.7 macrophages: role of iron. *Toxicol Lett*. 2006;165(1):88–100.
54. Donaldson K, Murphy F, Schinwald A, Duffin R, Poland CA. Identifying the pulmonary hazard of high aspect ratio nanoparticles to enable their safety-by-design. *Nanomedicine*. 2011;6(1):143–53.
55. Warheit DB, Laurence BR, Reed KL, Roach DH, Reynolds GAM, Webb TR. Comparative pulmonary toxicity assessment of single-wall carbon nanotubes in rats. *Toxicol Sci*. 2004;77(1):117–25.
56. Aiso S, Yamazaki K, Umeda Y, et al. Pulmonary toxicity of intratracheally instilled multiwall carbon nanotubes in male Fischer 344 rats. *Ind Health*. 2010; 48(6):783–95.